A Gm-C Anti-Aliasing Filter Design with Digitally Tunable Bandwidth for DVB-T Receivers[§]

Chua-Chin Wang[†], Ching-Li Lee, Chien-Chih Hung
Department of Electrical Engineering
National Sun Yat-Sen University
Kaohsiung, Taiwan 80424
ccwang@ee.nsysu.edu.tw

***Abstract*— This paper presents a temperature-compensated 6th order transconductance-C (Gm-C) anti-aliasing filter (AAF) with digitally tunable bandwidth which can be applied in the analog front-end circuit of DVB-T receivers. The proposed AAF is controlled by digital signals to provide three different baseband bandwidth (6, 7, 8 MHz). A regulator with band-gap circuitry supplies a stable voltage to suppress the variations of power and temperature. Moreover, a temperature-compensated circuitry is used to neutralize bandwidth drifting caused by the temperature variation. The bandwidth accuracy of the proposed design verified by HSPICE post-layout simulations is better than 3.28% at every PVT (process, supply voltage, temperature) corner which is adequate for the DVB-T receivers' baseband processing.**

I. Introduction

In the wireless communication systems, a mixer converts the analog front-end output signal into a signal that the baseband can process. The AAF is used to removes the adjacent-channel signals generated by the mixer to avoid inter-channel interferences [2] [3] [8]. Traditional RC-based filters with passive elements can not be directly applied in SOC (System-on-Chip) designs due to large area cost. Although operation amplifiers (OPAMP) can be used to replace large passive elements, e.g., inductors and capacitors, they are limited for high-frequency usages [4]. By contrast, transconductance amplifiers (OTA) have the following advantages : the transconductance varying with bias voltages, operating in a wide frequency range, high input impedance, and high output impedance. Besides, they can be used as large resistors given proper configurations. Hence, the Gm-C filter based on OTAs is better than the OPAMP-C filter regarding application in the SOC designs, [1], [5], [6], [7]. A 6th order Gm-C AAF is proposed in this work. The proposed AAF is implemented by 0.35 μm 2P4M CMOS technology process. The post-layout simulation reveals that the accuracy of the bandwidth is better than 3.28% at every PVT corner.

II. Gm-C AAF Design

A typical analog front-end of DVB-T receivers is shown in Fig. 1. The AAF receives mixer's output signal, and then selects the desired bandwidth by external digital control signals. Then, it converts the received signal into the input of the following AGC (automatic gain control) circuitry for further baseband signal processing.

A. AAF

Fig. 2 shows the basic AAF structure which is a 6th order passive LC ladder filter [2]. In order to carry out the feasibility, the passive inductors are replaced with active inductors, while the resistors are replaced with active Gm elements. Referring to Fig. 3, which is the architecture of Nauta's transconductor [1], the V-I transfer function of the transconductor is as follows.

$$\begin{aligned} I_{od} &= I_{o1} - I_{o2} \\ &= V_{id} \cdot (V_{DD} - V_{thn} + V_{thp}) \cdot \sqrt{\beta_n \cdot \beta_p} \\ &= V_{id} \cdot gm, \end{aligned} \tag{1}$$

where V_{id} is the differential input voltage, V_{thn} and V_{thp} are the threshold voltages of NMOS and PMOS transistors, respectively, β_n and β_p are the transconductance parameters of NMOS and PMOS transistors, respectively, and *gm* is the equivalent transconductance of Nauta's transconductor. The transconductor can be denoted as a single element, as shown in Fig. 4.

Passive inductors usually occupy large area on chip, which is not acceptable in SOC designs. Hence, we utilize the symmetrical floating gyrator in Fig. 5 instead, which is equivalent to an inductor [3]. The current at V_L is as follows.

$$-sC_LV_L - gmV_1 + gmV_2 = 0, \tag{2}$$

$$V_L = \frac{gm(V_1 - V_2)}{sC_L}, \tag{3}$$

where I_1 and I_2 are, respectively, given by

$$\begin{aligned} I_1 &= \frac{gm^2(V_1 - V_2)}{sC_L}, \\ I_2 &= \frac{gm^2(V_2 - V_1)}{sC_L}, \end{aligned} \tag{4}$$

The equivalent inductance, thus, is derived as follows.

$$L = \frac{V}{I} = \frac{C_L}{gm^2}, \tag{5}$$

[§]This research was partially supported by National Science Council under grant NSC 92-2220-E-110-001 and 92-2220-E-110-004.
[†] the contact author

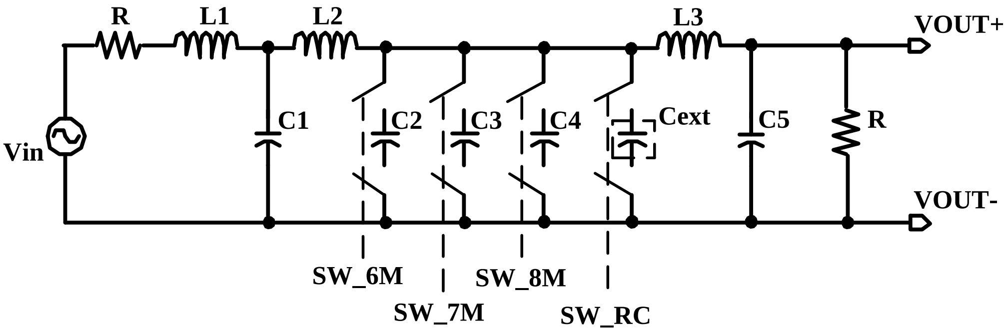

Fig. 2. 6th order passive LC ladder filter

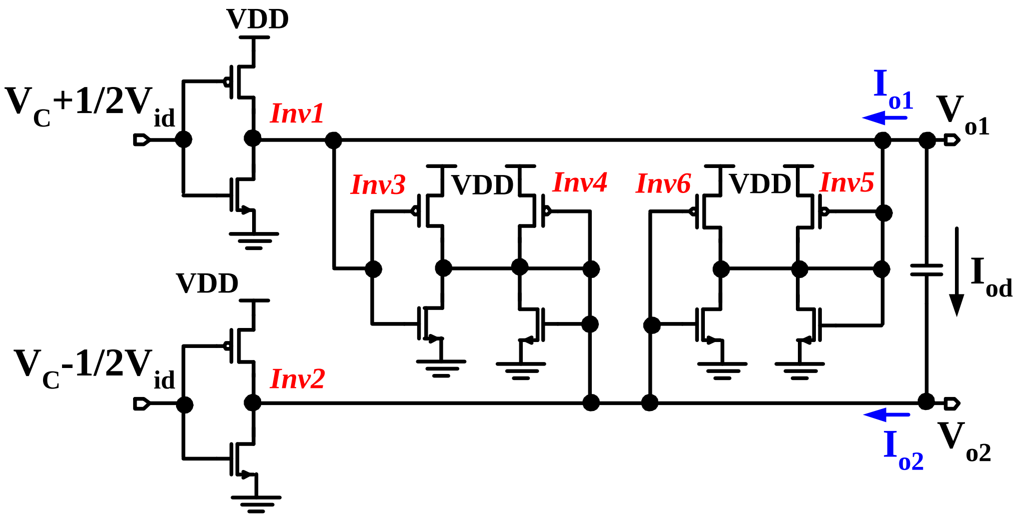

Fig. 3. Nauta's symmetric transconductor

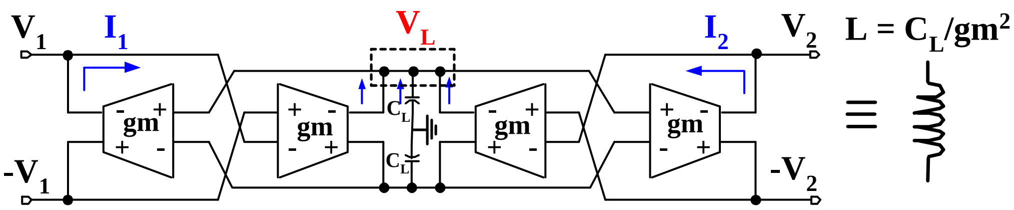

Fig. 5. Symmetrical floating gyrator which is equivalent to an inductor

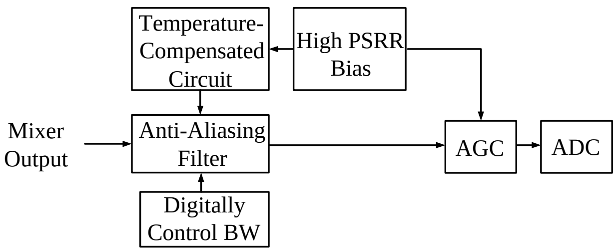

Fig. 1. Analog front-end of DVB-T receivers

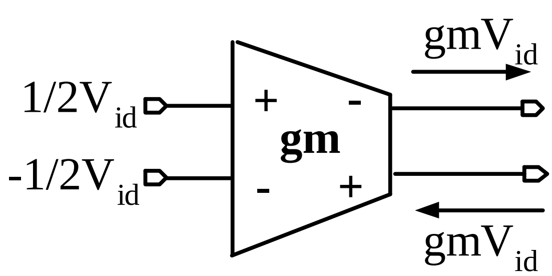

Fig. 4. Symbolic of the symmetric transconductor

The resistor can also be replaced with the symmetric transconductor of the Fig 4. Fig. 6 shows the equivalent circuit of the resistor.

$$R = \frac{V}{I} = \frac{V}{gm \cdot V} = \frac{1}{gm} \tag{6}$$

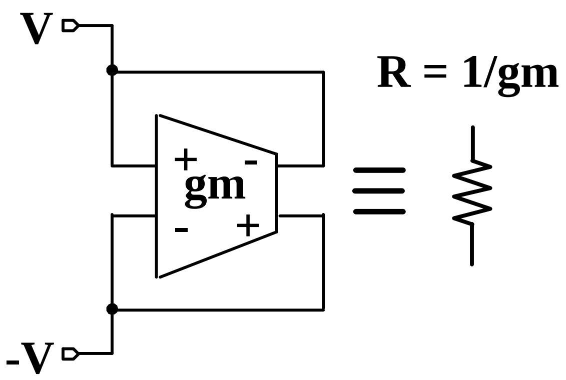

Fig. 6. Equivalent circuit of the resistor

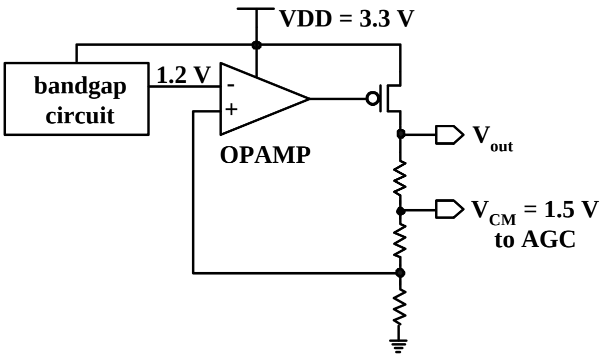

Fig. 8. High PSRR regulator

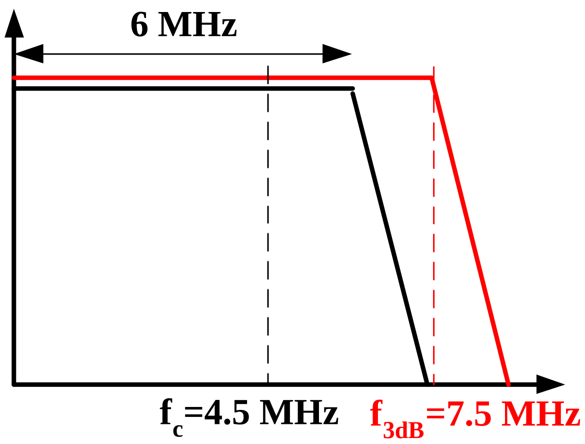

Fig. 7. DVB-T baseband spectrum with 6 MHz data bandwidth

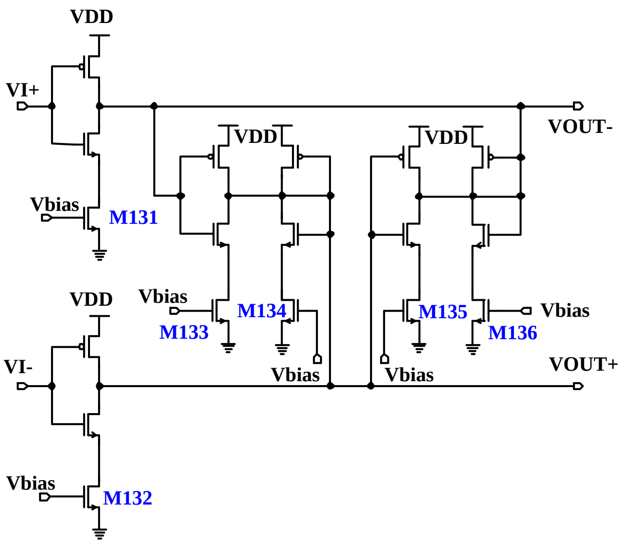

Fig. 9. Modified Nauta's symmetric transconductor

TABLE I

BANDWIDTH SELECTION TABLE

SW_6M	SW_7M	SW_8M	SW_RC	F_{3dB}
open	open	close	open	8.5 MHz
open	close	close	open	8.0 MHz
close	close	close	open	7.5 MHz
open	open	open	close	external capacitor

The DVB-T specifications [8] require three different baseband bandwidths: 6, 7, and 8 MHz. Therefore, the cut-off frequencies thereof are set to 7.5, 8.0, and 8.5 MHz, respectively. For example, Fig. 7 shows a DVB-T baseband spectrum with 6 MHz data bandwidth. In order to meet the requirements, the digital controlled switches, SW_6M, SW_7M, SW_8M in Fig. 2, are used in the AAF circuit such that the bandwidth of the output signal can be selected. Table I shows the bandwidth selection table. Notably, SW_RC is added to select an external RC filter for the proposed of testing.

B. High PSRR regulator

The Gm-C filter needs a stable bias to resist the variation of power supply voltage and temperature. Fig. 8 shows a high PSRR (power supply rejection ratio) regulator which is composed of a band-gap circuit, OPAMP, PMOS transistor, and a resistor string. The regulator provides a stable voltage to all of the AAF sub-circuits. Besides, a voltage divider composed of resistors supplies 1.5 V voltage to the AGC as the common mode voltage such that the following ADC can attain maximum input signal swing. The post-layout simulations prove that when the power supply voltage varies within ±15 %, the output voltage drift of the regulator is less than ±4 %.

C. Temperature-compensated circuit

The *gm* of the Nauta's symmetric transconductor varies with the temperature drifting, because there is no protection or compensation devices in the circuit. Consequently, the filtering bandwidth will be drifting, and unwanted noise might appear. Hence, a modified Nauta's symmetric transconductor structure as shown in Fig. 9 is employed. The NMOS transistors (M131 - M136), namely foot switches, are inserted between the GND and the pull-down NMOS in each inverter as a tail current control mechanism to limit the bias current. Then, the variation of the *gm*

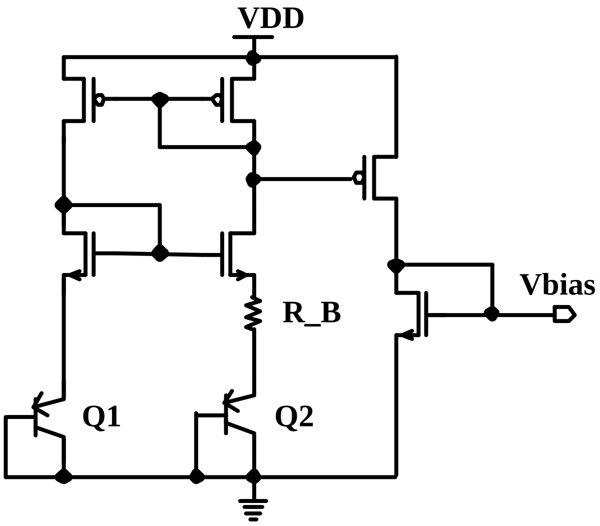

Fig. 10. Temperature-compensated circuit

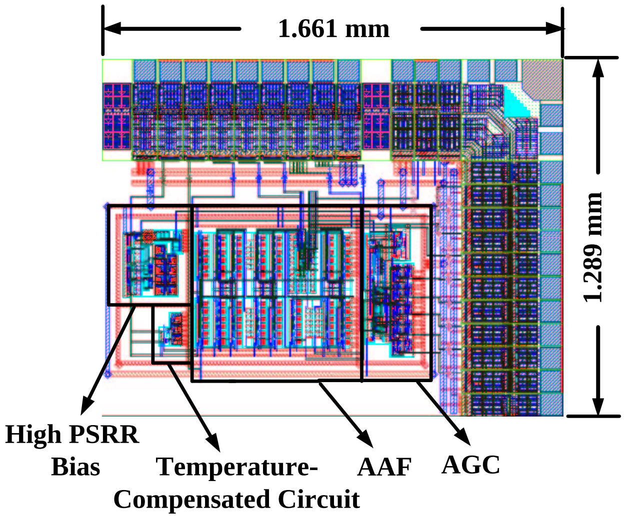

Fig. 11. Layout of the proposed AAF

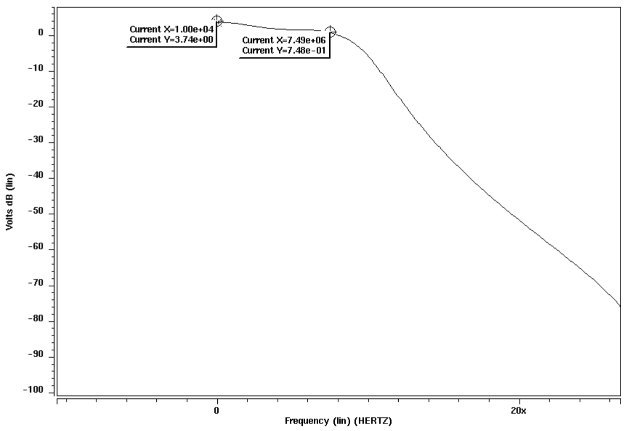

Fig. 12. Post-layout simulation of 6 MHz baseband bandwidth, at TT model, VDD = 3.3 V, 25^{o}C

as well as the filtering bandwidth is reduced. The V_{bias} voltage in Fig. 9 is generated by a temperature-compensated circuit shown in Fig. 10. In order to cancel the effect of temperature variation, the R_B with a positive temperature coefficient can be appropriately tuned to compensate the variation of the *gm*.

III. Simulation and Implementation

TSMC (Taiwan Semiconductor Manufacturing Company) 0.35 μm 2P4M CMOS process is adopted to carry out the proposed design. Fig. 11 shows the layout of the proposed design. Notably, all of the PVT corners are simulated. Fig. 12, 13, 14, show the post-layout simulations of the frequency response given 6, 7, 8 MHz baseband bandwidth, respectively, at TT model, VDD = 3.3 V, 25^{o}C. Given the 6 MHz baseband bandwidth with a 7.5 MHz cut-off frequency, all of the PVT corner simulation results are revealed in Fig. 15. The accuracy of the cut-off bandwidth is 3.28% in the worst-case. A comparison of the proposed design with several prior designs is summarized in Table II. Notably, we carry out the AAF with the least advanced process, but attain the best performance regarding the accuracy, the area and the normalized power dissipation.

IV. Conclusion

We have proposed a novel digitally tunable bandwidth Gm-C anti-aliasing filter for DVB-T receivers. The different channel bandwidth tuning can be carried out by digital control signals. Besides, the modified Nauta's symmetric transconductor is proposed to suppress the *gm* and filtering channel bandwidth variations with temperature drifting. The post-layout simulation results justify the advantages of the proposed AAF design.

References

[1] B. Nauta, "A CMOS transconductance-C filter technique for very high frequencies," *IEEE J. of Solid-State Circuits,* vol. 27, no. 2, pp. 142-153, Feb. 1992.

[2] K. Su, "Analog Filters," Reading : second edition, Kluwer Academic Publishers, 2002

[3] R. Schaumann, and M. E. V. Valkenburg, "Design of Analog Filters," Reading : published by Oxford University Press, Inc, 2001.

[4] B. Razavi, "Design of Analog CMOS Integrated Circuits," New York, McGraw Hill, 2002.

[5] S. Mehrmanesh, H. A. Aslanzadeh, M. B. Vahidfar, and M. Atarodi, "A 1.8V high dynamic range CMOS Gm-C filter for portable video systems," *2002 14th Inter. Conf. on Microelectronics (ICM'03),* pp. 38-41, Dec. 2002.

[6] L. Ramezani, "An adjustable bandwidth analog CMOS Gm-C filter," *2003 10th IEEE Inter. Conf. on Electronics, Circuits and Systems (ICECS'03),* vol. 2 , pp. 420-422, Dec. 2003.

[7] A. C. Carusone, and D. A. Johns, "A 5th order Gm-C filter in 0.25 um CMOS with digitally programmable poles and zeroes," *2002. IEEE Inter. Symp. on Circuits and Systems (ISCAS'02),* vol. 4 , pp. 635-638, May 2002.

[8] M. Massel, "Digital Television DVB-T COFDM and ATSC 8-VSB," Reading : published by digitalTVbooks.com, 2000.

TABLE II

COMPARISON WITH PRIOR DESIGNS

	[5]	[6]	[7]	ours
CMOS Process	0.25 μm	0.35 μm	0.25 μm	0.35 μm
VDD	1.8 V	$\pm$2.5 V	2.5 V	3.3 V
Cut-off freq.	5 MHz	1 - 2 MHz	8 MHz	7.5, 8, 8.5 MHz
Accuracy	4%	N/A	N/A	$\leq$ 3.28%
Area	N/A	N/A	2.5 mm^2	2.14 mm^2
Power	25 mW	34 mW	223 mW	33.58 mW

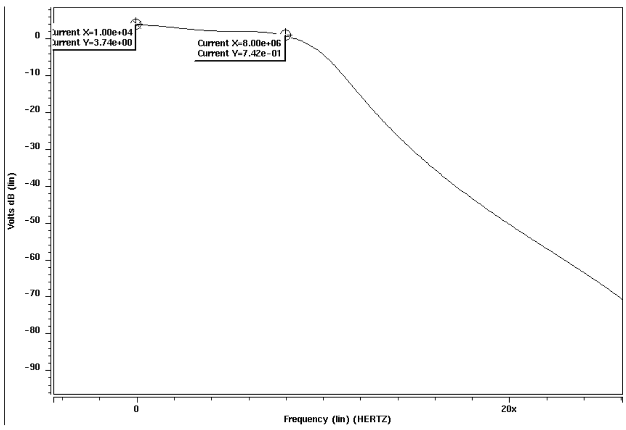

Fig. 13. Post-layout simulation of 7 MHz baseband bandwidth, at TT model, VDD = 3.3 V, 25^{o}C

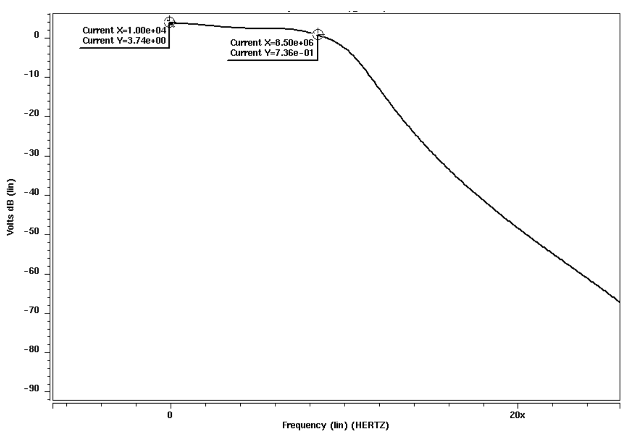

Fig. 14. Post-layout simulation of 8 MHz baseband bandwidth, at TT model, VDD = 3.3 V, 25^{o}C

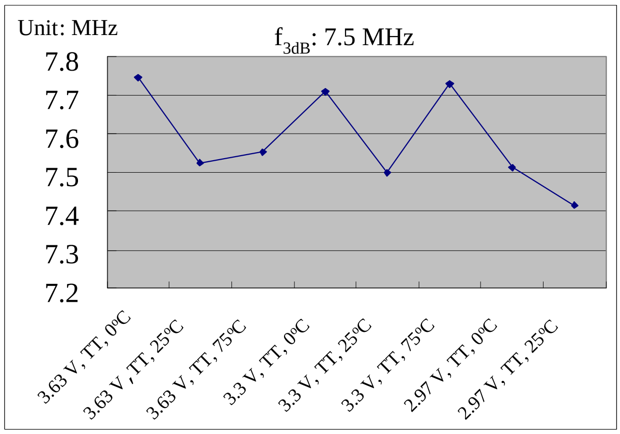

Fig. 15. Post-layout simulation of 6 MHz data bandwidth (all PVT corners)